

AEDC-TR-75-146

AFRPL-TR-75-61

cy. 2



DOC_NUM SER CN
UNC22521-PDC A 1



JAN 19 1976

1988

RAYLEIGH SCATTERING STUDIES OF CO₂ EXPANSION FLOW FIELDS

VON KÁRMÁN GAS DYNAMICS FACILITY
ARNOLD ENGINEERING DEVELOPMENT CENTER
AIR FORCE SYSTEMS COMMAND
ARNOLD AIR FORCE STATION, TENNESSEE 37389

December 1975

Final Report for Period July 1, 1974 — June 30, 1975

Approved for public release; distribution unlimited.

PROPERTY OF U. S. AIR FORCE
AEDC LIBRARY
F40600-75-C-0001

Prepared for

AIR FORCE ROCKET PROPULSION LABORATORY (DYSP)
EDWARDS AIR FORCE BASE, CALIFORNIA 93523

NOTICES

When U. S. Government drawings specifications, or other data are used for any purpose other than a definitely related Government procurement operation, the Government thereby incurs no responsibility nor any obligation whatsoever, and the fact that the Government may have formulated, furnished, or in any way supplied the said drawings, specifications, or other data, is not to be regarded by implication or otherwise, or in any manner licensing the holder or any other person or corporation, or conveying any rights or permission to manufacture, use, or sell any patented invention that may in any way be related thereto.

Qualified users may obtain copies of this report from the Defense Documentation Center.

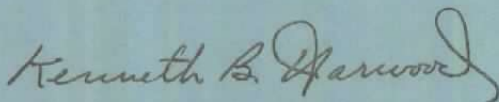
References to named commercial products in this report are not to be considered in any sense as an endorsement of the product by the United States Air Force or the Government.

This report has been reviewed by the Information Office (OI) and is releasable to the National Technical Information Service (NTIS). At NTIS, it will be available to the general public, including foreign nations.

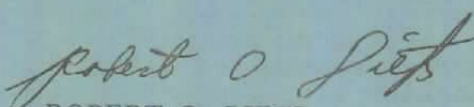
APPROVAL STATEMENT

This technical report has been reviewed and is approved for publication.

FOR THE COMMANDER



KENNETH B. HARWOOD
Captain, CF
Research & Development
Division
Directorate of Technology



ROBERT O. DIETZ
Director of Technology

UNCLASSIFIED

REPORT DOCUMENTATION PAGE		READ INSTRUCTIONS BEFORE COMPLETING FORM
1. REPORT NUMBER AEDC-TR-75-146 AFRPL-TR-75-61	2. GOVT ACCESSION NO.	3. RECIPIENT'S CATALOG NUMBER
4. TITLE (and Subtitle) RAYLEIGH SCATTERING STUDIES OF CO₂ EXPANSION FLOW FIELDS		5. TYPE OF REPORT & PERIOD COVERED Final Report - July 1, 1974 - June 30, 1975
		6. PERFORMING ORG. REPORT NUMBER
7. AUTHOR(s) W. D. Williams and J. W. L. Lewis ARO, Inc.		8. CONTRACT OR GRANT NUMBER(s)
9. PERFORMING ORGANIZATION NAME AND ADDRESS Arnold Engineering Development Center (DY) Arnold Air Force Station Tennessee 37389		10. PROGRAM ELEMENT, PROJECT, TASK AREA & WORK UNIT NUMBERS Program Element 62302F
11. CONTROLLING OFFICE NAME AND ADDRESS Arnold Engineering Development Center (DYFS) Arnold Air Force Station, Tennessee 37389		12. REPORT DATE December 1975
		13. NUMBER OF PAGES 23
14. MONITORING AGENCY NAME & ADDRESS (if different from Controlling Office)		15. SECURITY CLASS. (of this report) UNCLASSIFIED
		15a. DECLASSIFICATION/DOWNGRADING SCHEDULE N/A
16. DISTRIBUTION STATEMENT (of this Report) Approved for public release; distribution unlimited.		
17. DISTRIBUTION STATEMENT (of the abstract entered in Block 20, if different from Report)		
18. SUPPLEMENTARY NOTES Available in DDC		
19. KEY WORDS (Continue on reverse side if necessary and identify by block number) condensation expansion laser Rayleigh scattering Raman scattering		
20. ABSTRACT (Continue on reverse side if necessary and identify by block number) Sonic orifice expansions of CO₂ were investigated using laser Rayleigh scattering for detection of condensation onset within the expansion flow field. The axial region studied was 0.8 to 60 orifice diameters downstream of the orifice, and a range of reservoir pressures was employed for expansions of CO₂ at ambient temperature. Two sonic orifice sources, 1.325- and 3.2-mm diameter, were studied for the purpose of determining the appropriate reservoir scaling laws for condensation onset and growth. Rayleigh		

UNCLASSIFIED

UNCLASSIFIED

20. ABSTRACT (Continued)

scattering intensities are presented as a function of axial distance and reservoir pressure, and the results clearly show the regions of condensation onset and growth.

PREFACE

The work reported herein was conducted by the Arnold Engineering Development Center (AEDC), Air Force Systems Command (AFSC), under Program Element 62302F, at the request of the Air Force Rocket Propulsion Laboratory (AFRPL), AFSC. The AFRPL project monitor was Lt. I. L. Witbracht. The results were obtained by ARO, Inc. (a subsidiary of Sverdrup & Parcel and Associates, Inc.), contract operator of AEDC, AFSC, Arnold Air Force Station, Tennessee, under ARO Project Number V32S-51A. The authors of this report were W. D. Williams and J. W. L. Lewis, ARO, Inc. The manuscript (ARO Control No. ARO-VKF-TR-75-104) was submitted for publication on June 30, 1975.

CONTENTS

	<u>Page</u>
1.0 INTRODUCTION AND THEORY	
1.1 Background	5
1.2 Rayleigh Scattering	7
2.0 EXPERIMENTAL APPARATUS AND METHOD	
2.1 Gas Source and Vacuum Chamber	8
2.2 Rayleigh Scattering Apparatus	9
3.0 RESULTS AND DISCUSSION	11
4.0 CONCLUSIONS	20
REFERENCES	21

ILLUSTRATIONS

Figure

1. Schematic of 4- by 10-ft Research Chamber	9
2. Schematic of 4- by 10-ft Research Chamber Experimental Arrangement	10
3. Polarization Direction Diagram	10
4. Axial Variation of Scattered Intensity (I_s/I_o) at $P_o = 50$ and 77.7 torr	12
5. Axial Variation of Scattered Intensity (I_s/I_o) at $P_o = 100$ and 155.4 torr	13
6. Axial Variation of Scattered Intensity (I_s/I_o) at $P_o = 200$ and 310.8 torr	14
7. Axial Variation of Scattered Intensity (I_s/I_o) at $P_o = 250$ and 388.5 torr	15
8. Axial Variation of Scattered Intensity (I_s/I_o) at $P_o = 350$ and 543.9 torr	16
9. Axial Variation of Scattering Function $f_{(P_o)}^{(D)}$	18
10. Variation of Supersaturation Parameters (S_ϕ and S'_ϕ) with P_o	19

<u>Figure</u>	<u>Page</u>
11. Variation of Supersaturation Parameters (S_ϕ and S'_ϕ) with P_o	20
NOMENCLATURE.	22

1.0 INTRODUCTION AND THEORY

1.1 BACKGROUND

The number of previous studies of CO_2 condensation phenomena in gas dynamic expansion flow fields is indicative of the variety of applications requiring an understanding of the process. Among such applications, one finds the expansion of combustion products which frequently include CO_2 and, also, the production of high-speed flow fields of air which naturally contains CO_2 as a significant constituent. Previous studies have utilized a wide variety of flow diagnostic techniques which have been selected in some cases because of the intended application of the results.

As an example, Hagena and Obert (Ref. 1) have employed a mass spectrometric-retarding potential technique for studying the cluster size distribution of the far-field region of CO_2 expansions. Further mass spectrometric studies are exemplified by the work of Bailey (Ref. 2), in which not only are the species mass selected but also flow speed measurements are performed enabling one to obtain estimates of condensate mass fraction. However, once again it is the expansion far-field region which is studied, for at higher flow field densities it is recognized that skimmer interaction effects do exist (Ref. 2) and that the existence of a mild shock at the skimmer may be sufficient to dissociate the rather fragile clusters.

Beylich (Ref. 3) has used the electron beam fluorescence technique to study the density and rotational temperature of CO_2 plume expansions, but the application was particularly tortuous, for the CO_2 fluorescence spectra were not fully resolved and rotational temperatures are determined using the emission band profile. Further, in the region of condensation onset and growth, the gas density is sufficiently large to require significant collision quenching corrections.

Additional studies of CO_2 cluster properties have been performed most notably by French workers using the electron diffraction technique, and the work of Audit (Ref. 4) is typical of these efforts. The fundamental data of clusters provided by this technique include equilibrium, intermolecular bonding distances of the cluster, and possibly the cluster temperature. However, the diagnostic technique taken alone is lacking in the basic gas dynamic data which are necessary to unambiguously determine the cluster size. Further, the technique is a far-field, low-density experimental tool which suffers from the same disadvantages as does mass spectroscopy.

Finally, Rayleigh scattering has been successfully employed by Beylich (Ref. 5) and Lewis and Williams (Refs. 6 and 7) to observe the condensation onset and growth regions of a gas dynamic expansion process. The work of Refs. 6 and 7 extended the use of the technique to include observations of scattering depolarization factors and thereby deduce informative data regarding cluster asymmetry characteristics. It should also be noted that the work of Refs. 6 and 7 approached the scattering process from a molecular rather than macroscopic basis as did Beylich, and this approach has enabled fundamental information to be obtained regarding the accretion process of cluster formation.

More recently, the work of Lewis and Williams (Ref. 8) has demonstrated the application of Raman scattering to condensing flow field studies, thereby providing a means of measuring local values of both gas density and temperature. It is to be noted that, contrary to the techniques of Refs. 1 through 4, both Rayleigh and Raman scattering are applicable to the high-density regions of the flow field which are most convenient for condensation studies.

Despite the previous interest in CO_2 as described in Refs. 1 through 5 and the references quoted therein, little direct information exists regarding the spatial location within the flow field of condensation onset, or the degree of supersaturation capable of CO_2 and, also, the rate of growth of the clusters following condensation initiation. Further, general scaling laws for various types of gas sources such as sonic orifices and conical nozzles have not been verified. It should be noted that CO_2 presents a particularly challenging case: not only must condensation be considered, but also, for very modest reservoir temperatures, sufficient vibrational mode excitation exists to require consideration of vibrational relaxation phenomena as well. Consequently, prediction of the uncondensed gas dynamic expansion of CO_2 , which determines the detailed behavior of the condensation process at onset, is not a trivial problem.

The data of this report present the results of a study of Rayleigh scattering of the CO_2 monomers and clusters produced by a sonic orifice expansion from ambient temperature reservoir conditions. Because of the complexity of the study, further work is both in progress and planned, and it is hoped that the results and analysis of CO_2 expansions will be presented in more completeness in following reports.

1.2 RAYLEIGH SCATTERING

The basic equations and rationale for the application of Rayleigh scattering to the study of condensing gas flow fields have been presented and discussed in previous publications (Refs. 6 and 7). Consequently, only a summary of the pertinent information and equations will be given in this section.

It will be recalled from Refs. 6 and 7 that for an incident polarized laser source of wavelength (λ) and intensity (I_0) interacting with a gas sample of number density (N_1) the Rayleigh scattered intensity (I_s) can be written as

$$I_s/I_0 = (K_a/\lambda^4) N_0 \alpha_1^2 (N_1/N_0) \quad (1)$$

where α_1 is the molecular polarizability, N_0 is the gas reservoir density and K_a is a constant including optical, geometrical, and fundamental atomic constants. If the flow field is isentropic, obviously I_s/I_0 is a direct measure of the isentropic density ratio $(N_1/N_0)^0$, where the superscript zero denotes isentropic conditions. As shown in Refs. 6 and 7 for a condensing flow field consisting not only of monomers (denoted by the subscript one) but also clusters, or i-mers (denoted by subscript i), the scattered intensity can be written as

$$[(I_s/I_0)/(I_s/I_0)^0] - (N_1/N_1^0) = (N_T/N_1^0) \cdot X_c \cdot \sum_{i=2}^{\infty} p(i) \cdot (a_i/a_1)^2 \quad (2)$$

where N_T is the local total number density, X_c is the condensate mole fraction and $p(i)$ is the probability distribution function of the i-mer. If one approximates N_1/N_1^0 and N_T/N_1^0 by unity and then defines the left-hand side of Eq. (2) as the scattering function f , one finds

$$f \approx X_c \sum_{i=2}^{\infty} p(i) (a_i/a_1)^2 \quad (3)$$

Further, assuming weak van der Waal's binding of the clusters, one can approximate a_i as

$$a_i \approx i a_1 \quad (4)$$

i. e., cluster polarizability is assumed to be additive. Then

$$f \approx X_c \sum_{i=2}^{\infty} i^2 p(i) \quad (5)$$

For a monodisperse distribution,

$$\begin{aligned} p(i) &= 1 & i &= J \\ &= 0 & i &\neq J \end{aligned}$$

Then,

$$f \approx X_c \cdot J^2 \quad (6)$$

so, if knowledge of the mole fraction can be obtained, cluster size J follows.

Obviously, prior to condensation onset, f is zero identically, and positive deviations of f from zero are indicative of the initiation of clustering. Further, the parameter J of Eq. (6) will be a space-dependent quantity throughout the condensation growth region, as will X_c , and f is an ambiguous measure of the increase in the mean cluster size and mole fraction of condensate.

The results presented in this report will be the variation of the scattering function f with various experimental parameters. The condensation onset and growth regions will be clearly shown as will an important orifice diameter/reservoir pressure scaling law.

2.0 EXPERIMENTAL APPARATUS AND METHOD

2.1 GAS SOURCE AND VACUUM CHAMBER

The sonic orifice sources were of 1.325- and 3.2-mm diameter with a diameter-to-thickness ratio greater than 20. The orifice was located at the end of a tubular, stainless-steel reservoir of approximately 1-cm inner diameter, and equilibration of the gas and tube wall temperatures was ensured. Reservoir temperature and pressure were measured using calibrated transducers, and the flow-field data were acquired using Coleman grade CO_2 . Two $0.025\text{-}\mu\text{m}$ particulate filters were located in the inlet gas line to minimize heterogeneous condensation processes. The gas source was mounted on a traversing mechanism to provide three degrees of freedom and to enable flow field measurements to be made using fixed optical instrumentation. The movement mechanism has an accuracy and reproducibility of 0.013 cm in the axial direction.

The 4- by 10-ft Research Vacuum Chamber enclosing the motor-driven traversing mechanism, as shown in Fig. 1, was cryopumped using liquid N_2 and 20 K gaseous He. Background pressures of less than 10^{-5} torr were maintained for the maximum flow rate investigated. Pressure and temperature fluctuations in the reservoir were negligible. A more complete description is to be found in Ref. 6.

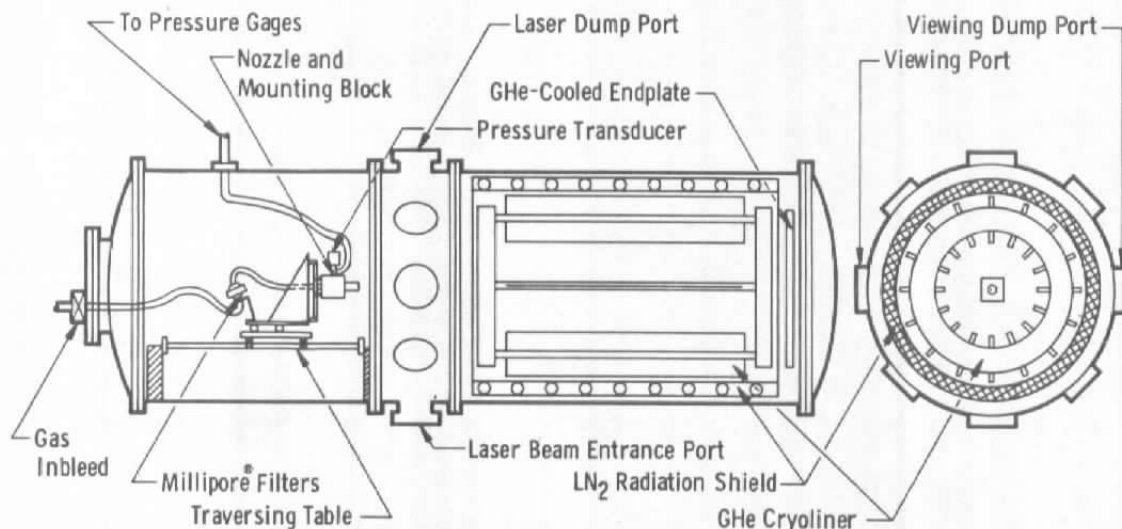


Figure 1. Schematic of 4- by 10-ft Research Chamber.

2.2 RAYLEIGH SCATTERING APPARATUS

The optical and electronic configurations of the experimental apparatus are shown in Fig. 2, and the polarization vector orientation for this scattering study is shown in Fig. 3. An argon ion laser of 1.0 w intensity at 514.5 nm was employed as the incident radiation source. The collection optics train included, in addition to collection and focusing lenses, a half-wave plate polarization rotator, and HN-22 Polaroid® for definition of the state of polarization of the scattered radiation. The system, which is described in detail in Ref. 8, utilized a Spex 1402 double spectrometer with two ganged 102- by 102-mm gratings of 1200 grooves/mm and blazed at 500.0 nm. The focal length of the instrument was 0.85 m with a reciprocal linear dispersion of approximately 0.44 nm/mm. The three slit widths were set at 200, 400, and 400 μ m in order of input to output slits. Photon counting electronics in conjunction with a thermoelectrically cooled photomultiplier tube served for data acquisition. The experimental procedures and method used are presented in Refs. 7 and 8.

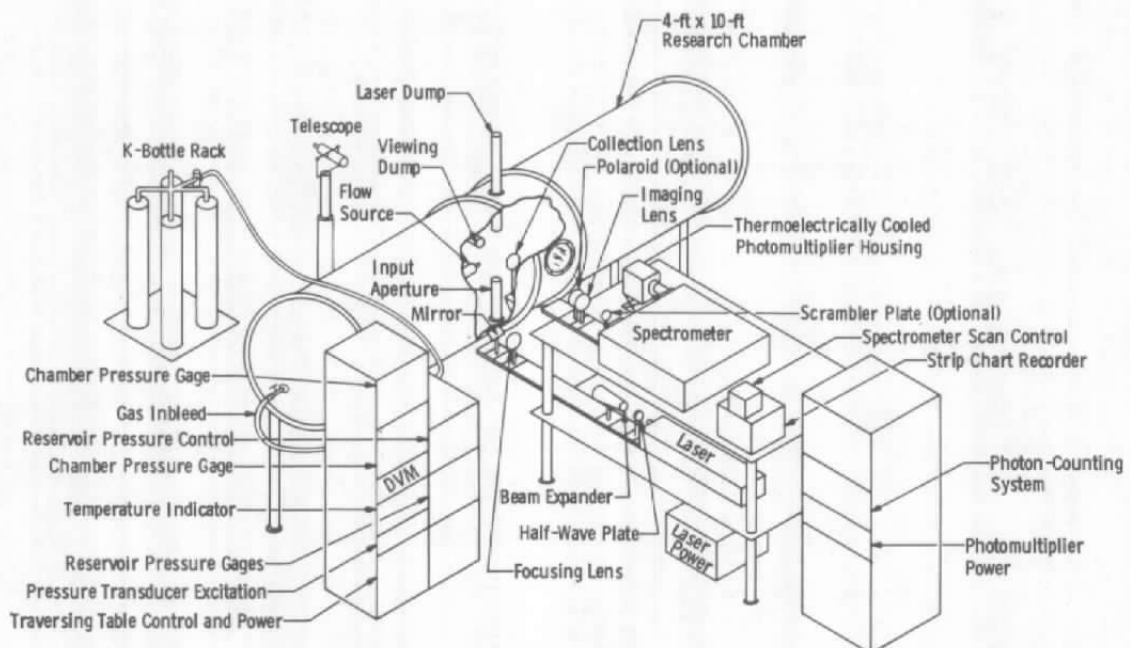


Figure 2. Schematic of 4- by 10-ft Research Chamber experimental arrangement.

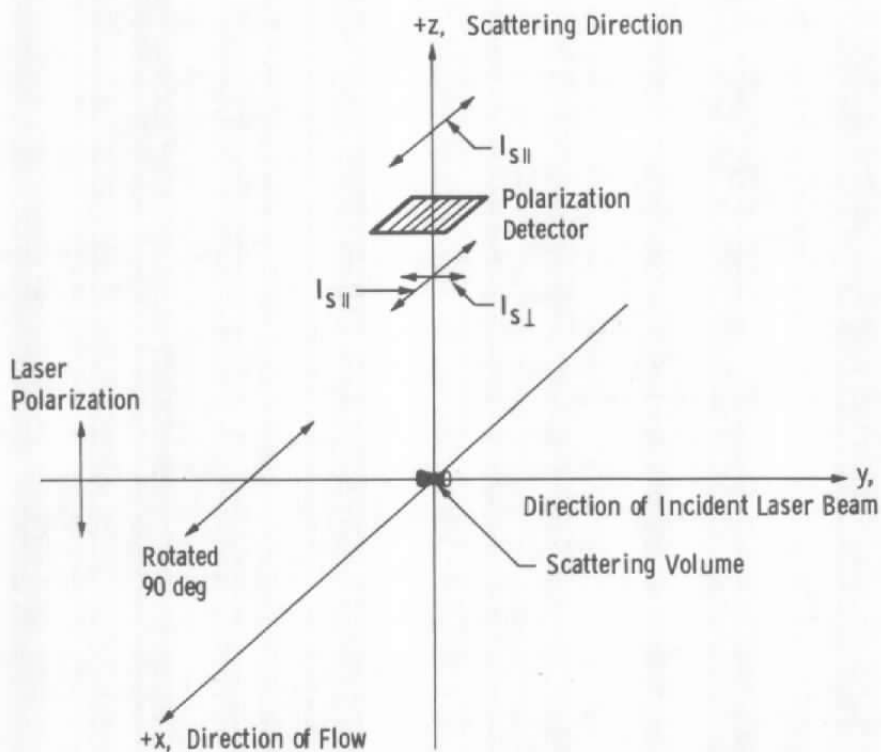


Figure 3. Polarization direction diagram.

3.0 RESULTS AND DISCUSSION

Sonic orifice expansions of CO₂ were produced using source diameters (D) of 1.325 and 3.2 mm. The reservoir pressure (P₀) was varied over the range of 50 to 350 torr for the 3.2-mm-diam source, and for the 1.325-mm-diam source, the P₀ range was 77.7 to 543.9 torr. The values of P₀ for the smaller diameter source were selected to achieve constant values of P₀²D for the two sources at each value of P₀ studied. The axial variation of the Rayleigh scattered intensity was determined over the axial distance range of 0.8 ≤ x/D ≤ 60 where x is the axial distance measured downstream from the flat-faced sonic orifice source. All cases studied were for ambient CO₂ reservoir temperature, which was nominally 280 K. Shown in Figs. 4 through 8 are the experimental Rayleigh scattering results for this study, and the ordinate is (Ref. 6):

$$I_s/I_0 = (K_a N_0 a_1^2 / \lambda^4) \cdot (N_T/N_0) \cdot \left[(N_1/N_T) + \sum_{i=2}^{\infty} (a_i/a_1)^2 (N_i/N_0) \cdot (N_0/N_T) \right] \quad (7)$$

where $K_a a_1^2 / \lambda^4$ is determined experimentally by an in situ calibration. It is seen from Eq. (7) that in the event of no condensation I_s/I_0 will vary directly as N_1/N_0 which, in the absence of vibrational relaxation effects, is the isentropic variation $(N_1/N_0)^0$. Also shown in Figs. 4 through 8 is the isentropic variation of N_1/N_0 as given by the Ashkenas-Sherman (Ref. 9) equations for $\gamma = 1.4$. The three-term expansion of Ref. 9 was used to enable accurate calculations for the axial distance region of $x/D \geq 1.0$. The axial locations at which saturation occurs $[(x/D)_s]$ were estimated for CO₂ using the data of Ref. 10 and assuming an isentropic expansion of CO₂ characterized by a specific heat ratio (γ) of 1.40. Differences of approximately ±20 percent in $(x/D)_s$ result from a variation in γ of approximately ±5 percent. More accurate values of $(x/D)_s$ are not required for this report, and it was found that for all cases studied

$$(x/D)_s \leq 0.4 \quad (8)$$

Consequently, the rate equations which describe the onset and growth regions of CO₂ must be applicable in the near field of the expansion.

It is seen from Fig. 4 that the expansion with the lowest P₀ yielded agreement with the $\gamma = 1.40$ isentropic prediction of Ref. 9 for $x/D \gtrsim 3$. Further, from Figs. 4 through 8, one sees that an increase in P₀ resulted in condensation onset and that the onset location decreased while the magnitude of deviation of I_s/I_0 from the isentropic dependence increased as P₀ increased.

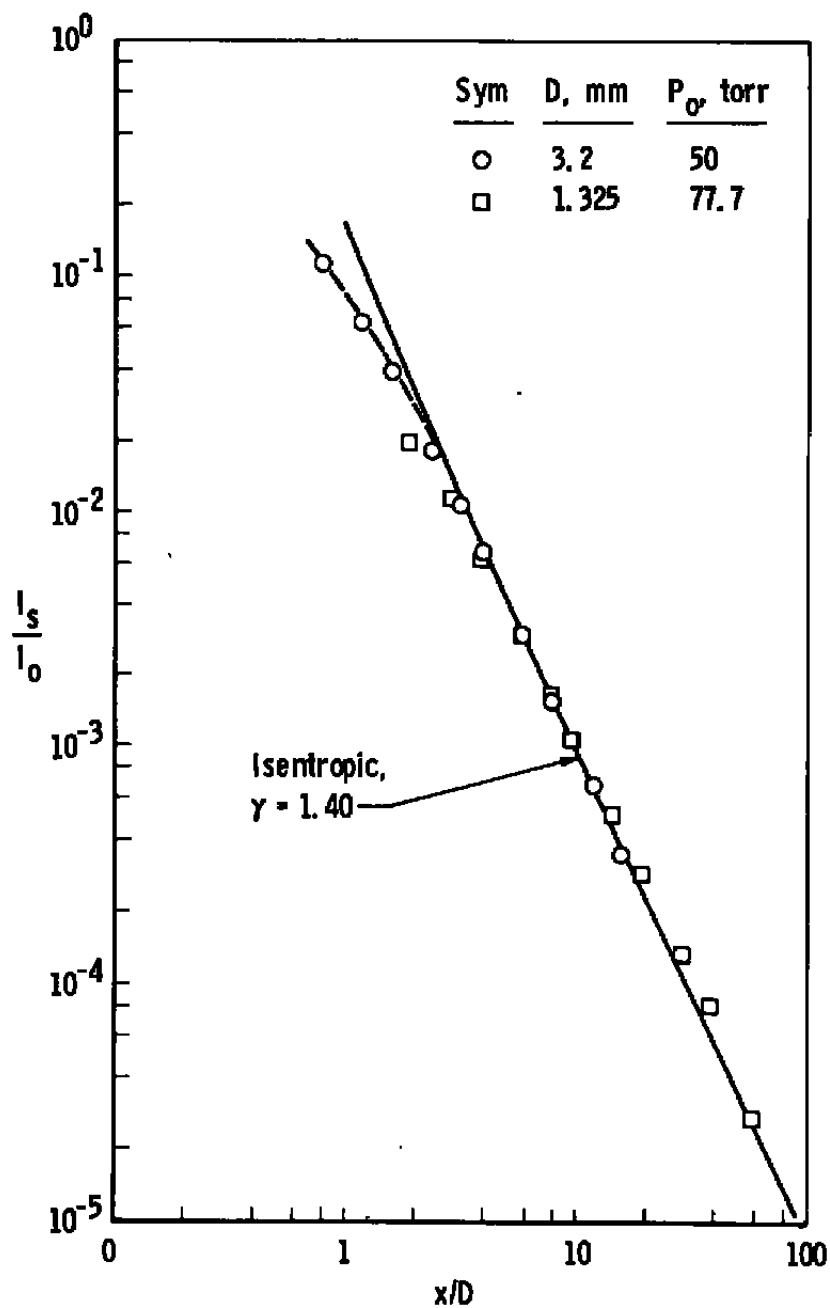


Figure 4. Axial variation of scattered intensity (I_s/I_0) at $P_0 = 50$ and 77.7 torr.

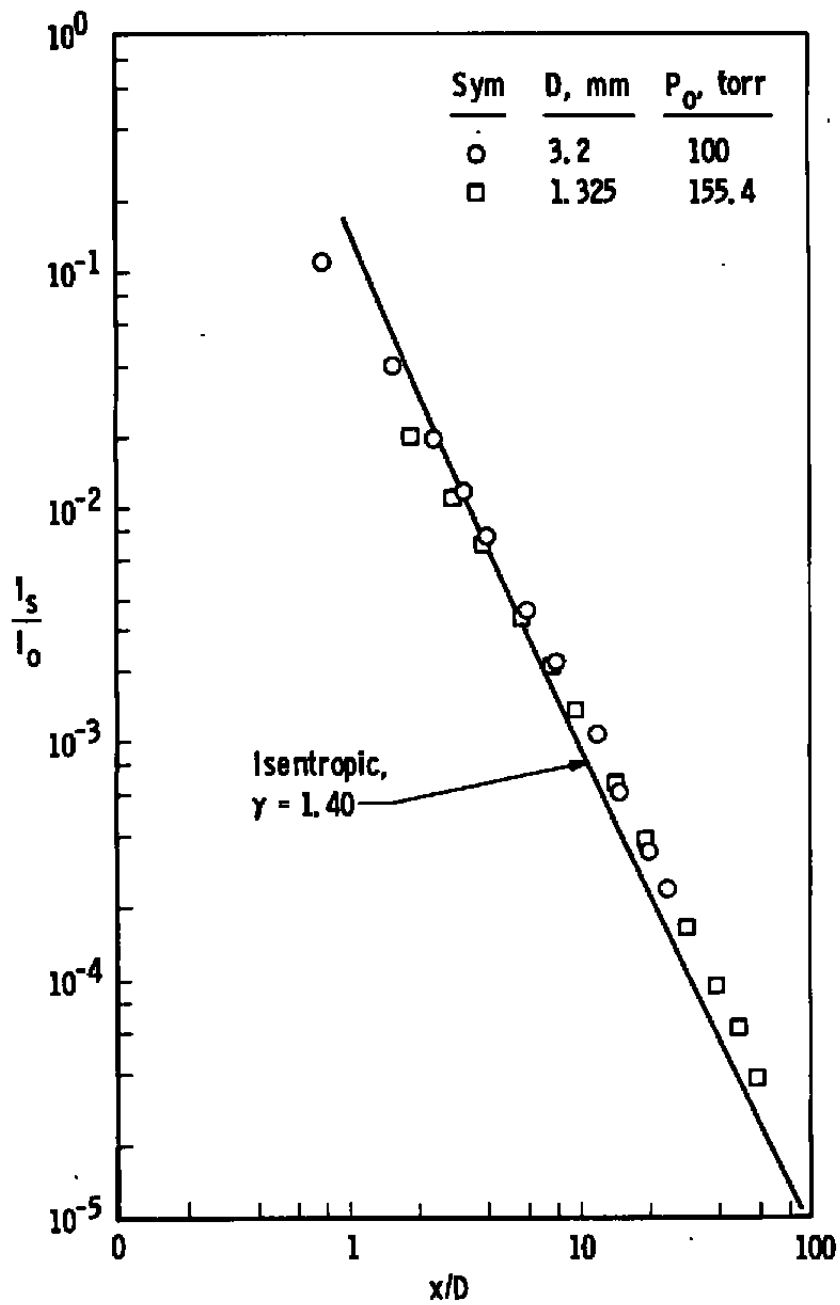


Figure 5. Axial variation of scattered intensity (I_s/I_0) at $P_0 = 100$ and 155.4 torr.

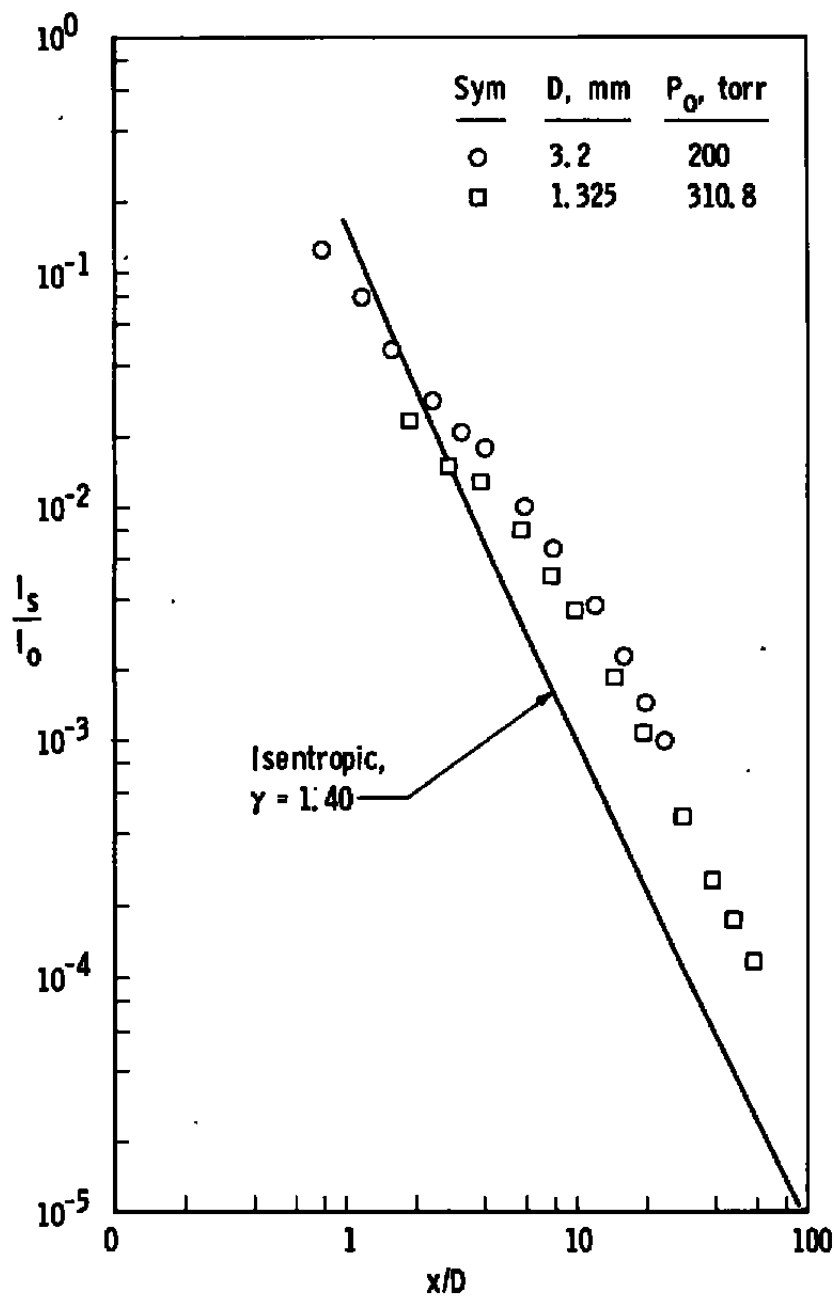


Figure 6. Axial variation of scattered intensity (I_s/I_0) at $P_0 = 200$ and 310.8 torr.

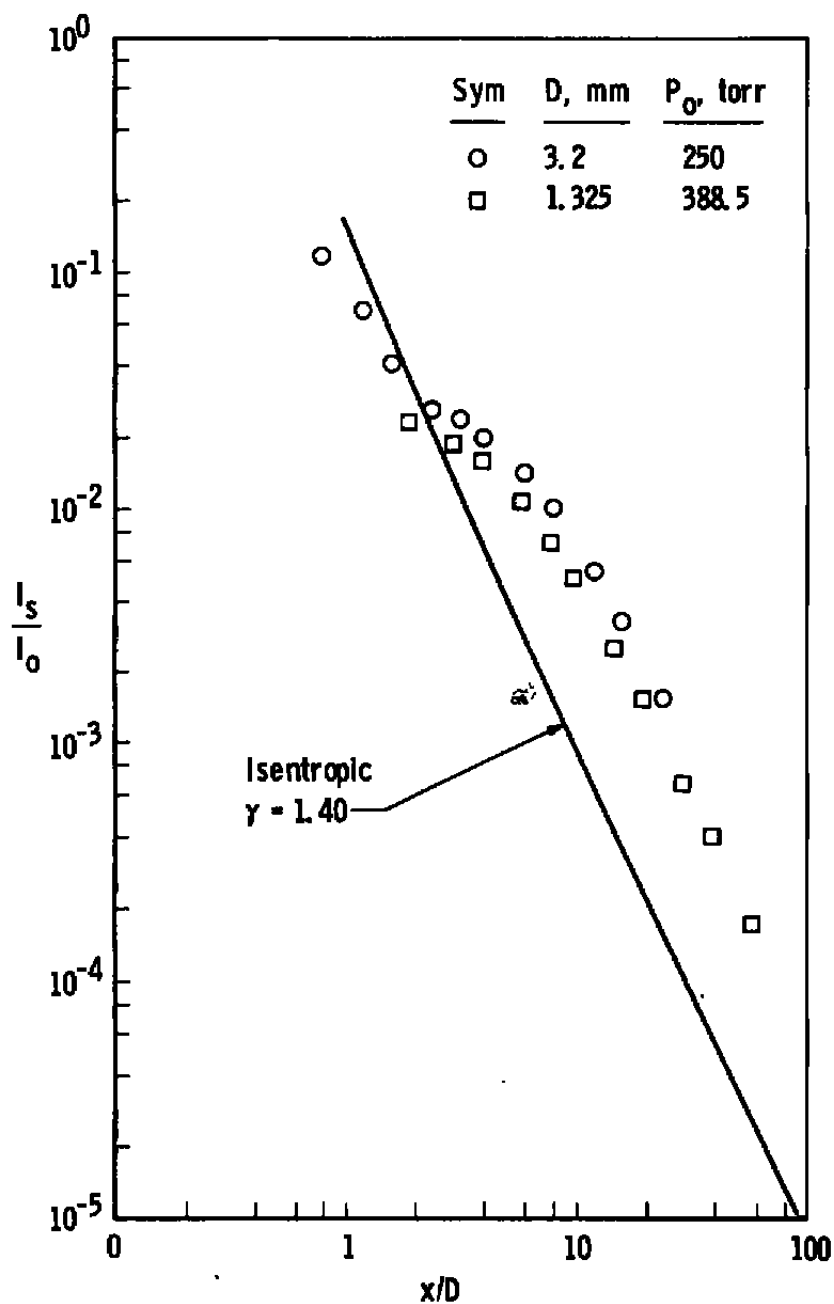


Figure 7. Axial variation of scattered intensity (I_s/I_o) at $P_o = 250$ and 388.5 torr.

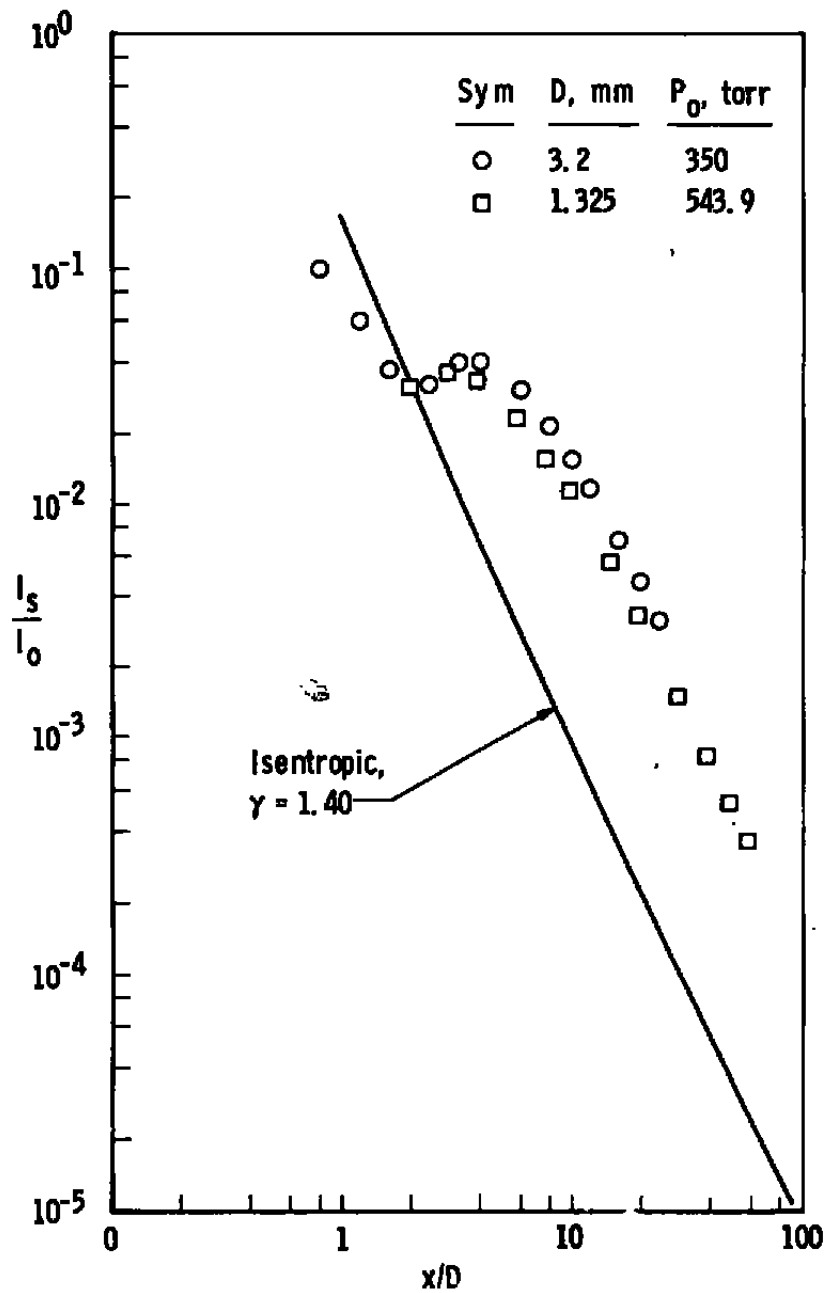


Figure 8. Axial variation of scattered intensity (I_s/I_0) at $P_0 = 350$ and 543.9 torr.

Additionally, one notes that, although the data from the two sonic orifice sources are in approximate agreement for constant values of $P_0^2 D$, there is an observable discrepancy in these data. Consequently, $P_0^2 D$ scaling yields an approximate scaling law for CO_2 , but further refinements are required to the scaling law to reduce the existing discrepancy.

The scattering function $f(P_0^{(D)})$ where the superscript and subscript denote the orifice diameter and reservoir pressure, respectively, is shown in Fig. 9 as a function of P_0 for the 3.2-mm-diam source. The rapid increase in f following onset is quite obvious as are the orders of magnitude increase in f as the reservoir pressure increases. The quantitative definition of condensation onset can take several forms. Used in this work are two criteria which involve either the scattering function f or the scattered intensity (I_s/I_0). The first method employs the criterion of a ten percent increase of I_s/I_0 relative to its isentropic value, and all condensation parameters derived using this criterion are denoted by the subscript ϕ . The second method uses the f function; and specifically, the variation of f with x/D is used to extrapolate the f function to the onset location. The value of the condensation parameters appropriate to this extrapolated axial position at which f equals zero are denoted by the subscript θ . Then the supersaturation parameters S and S' are defined as

$$S_{\theta,\phi} = T_s - (T_\infty)_{\theta,\phi} \quad (9)$$

and

$$S'_{\theta,\phi} = P_s / (P_\infty)_{\theta,\phi} \quad (10)$$

where the subscript ∞ denotes free-stream values. Figures 10 and 11 show the dependence of the supersaturation parameters on reservoir pressures for the two sonic orifice sources. From Figs. 10 and 11, it is seen that the temperature supercooling values determined from S_θ and S_ϕ are not substantially different and are on the order of 100 K. The locus of the saturation temperature T_s with P_0 is shown in Fig. 10. The variation of the pressure supersaturation ratios is seen to decrease significantly as P_0 increases.

Finally, empirical functional relations of f with axial distance X/D , $(X/D)_\theta$, P_0 , and D were obtained using the results of the axial variation of the scattering function data.

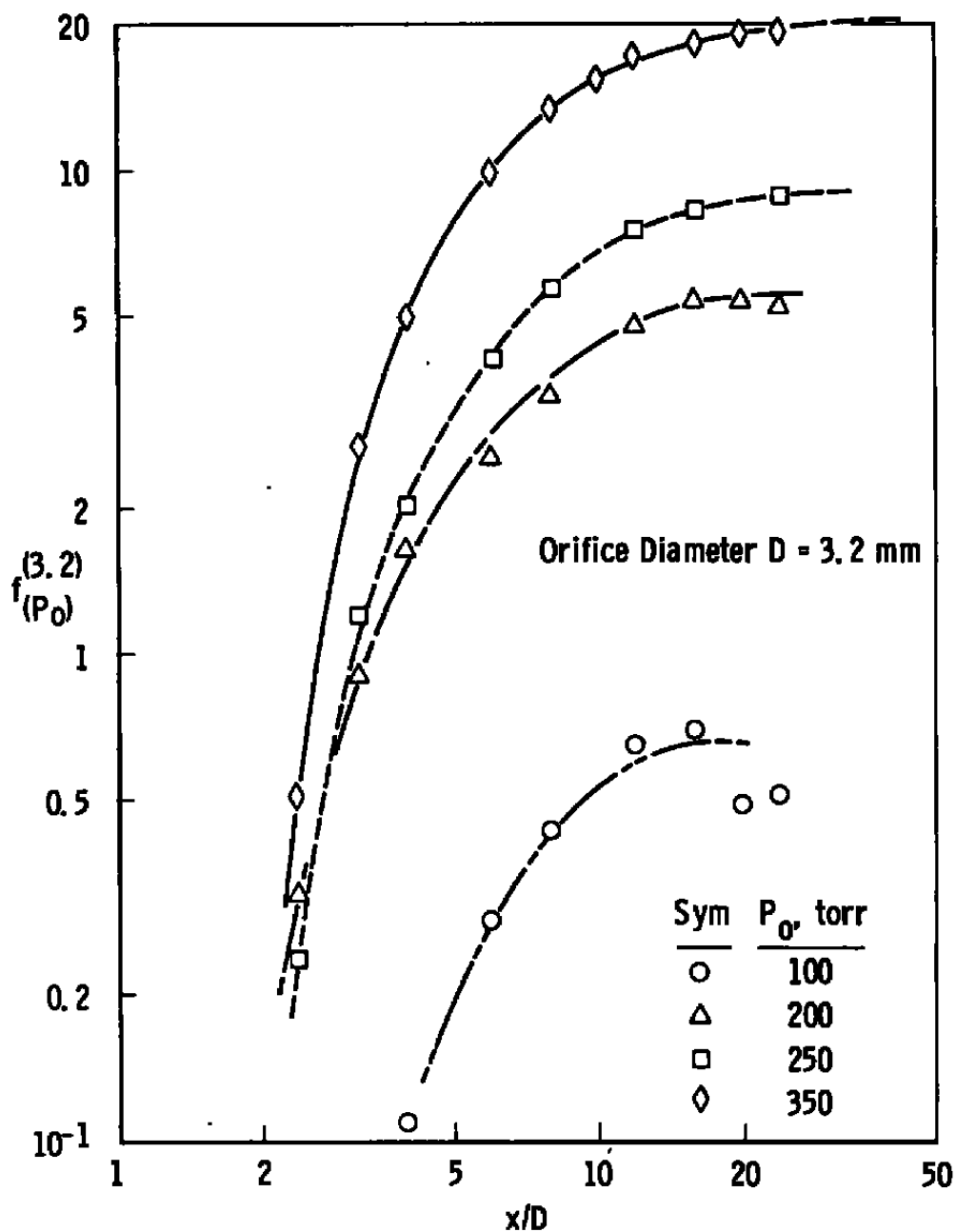


Figure 9. Axial variation of scattering function $f_{(P_0)}^{(D)}$.

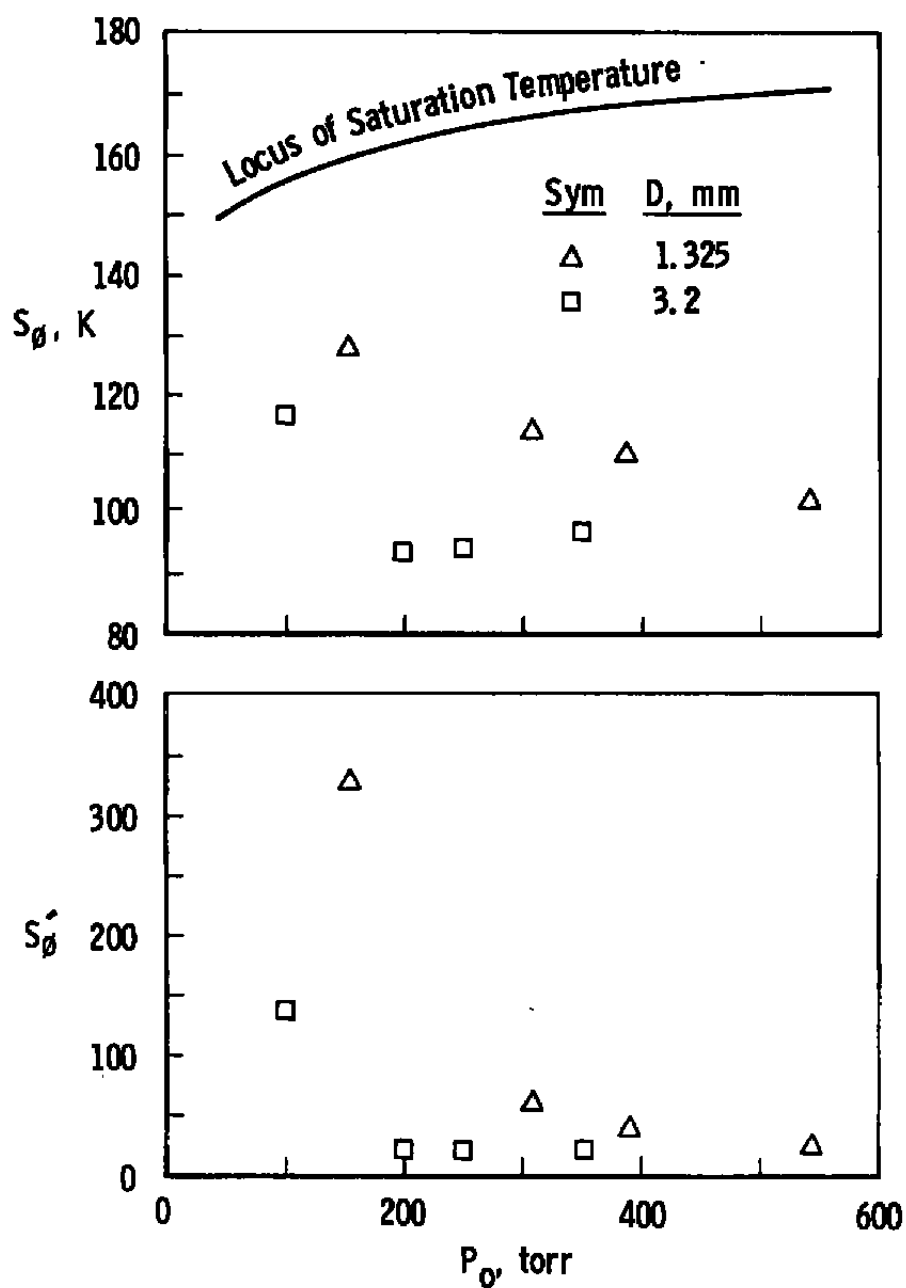


Figure 10. Variation of supersaturation parameters (S_ϕ and S'_ϕ) with P_0 .

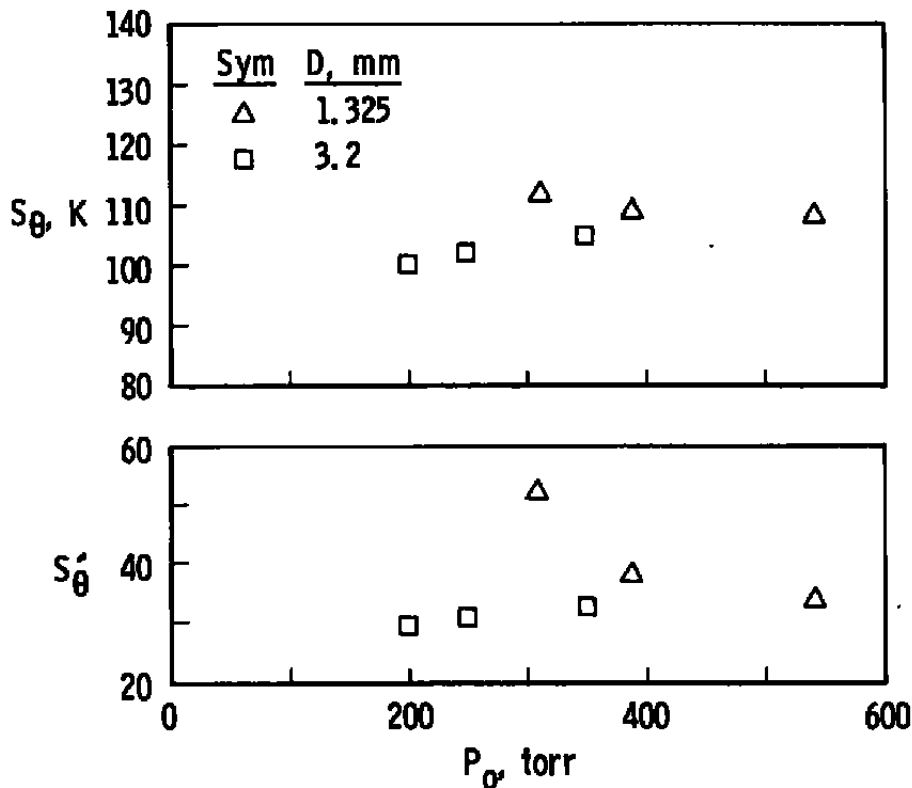


Figure 11. Variation of supersaturation parameters (S_θ and S'_θ) with P_0 .

The result found for the cases studied in the onset region is

$$f_{(P_0)}^{(D)} = b \ln [(X/D)/(X/D)_\theta] \quad (11)$$

where

$$b = C_0 / (D^{1.43} \cdot P_0^{2.20}) \quad (12)$$

and C_0 is a constant. After cessation of growth, the scattering function was found to be described by

$$f_{(P_0)}^{(D)} = P_0^{2.29} D^{1.62} / C_1 \quad (13)$$

where C_1 is a constant.

4.0 CONCLUSIONS

The results of Rayleigh scattering measurements of CO_2 sonic orifice expansions have demonstrated the onset of condensation and subsequent cluster growth as well as the very large increase in the scattering function (f) with increasing reservoir pressure. The results

for very low P_0 and uncondensed CO_2 indicate that the far-field expansion region is described by the isentropic, $\gamma = 1.4$ predictions of Ref. 9. However, for all cases studied, the saturation, onset, and growth regions for condensation all occur in the more complicated region of the expansion where the flow-field is yet developing, not in the far-field region of the expansion where one may use various asymptotic relations for the gas dynamic parameters. Empirical relations of the scattering function dependence on P_0 , D , and X/D were found and will serve as a basis for predicting gross condensation characteristics.

REFERENCES

1. Hagen, O. F. and Obert, W. "Cluster Formation in Expanding Supersonic Jets: Effect of Pressure, Temperature, Nozzle Size, and Test Gas." The Journal of Chemical Physics, Vol. 56, No. 5, March 1972, pp. 1793-1802.
2. Bailey, A. B. "Effects of Condensation of Gas Velocity in a Free-Jet Expansion." AEDC-TR-73-93 (AD762503), June 1973.
3. Beylich, A. E. "Experimental Investigation of Carbon Dioxide Jet Plumes." The Physics of Fluid, Vol. 14, May 1971, pp. 898-905.
4. Audit, P. "Liasons Intermoléculaires dan les Jets Supersoniques Etude par Diffraction d'Electrons." Journal Physique, Vol. 30, 1969, pp. 192-202.
5. Beylich, A. E. "Condensation in Carbon Dioxide Jet Plumes." AIAA Journal, Vol. 8, May 1970, pp. 965-967.
6. Lewis, J. W. L., and Williams, W. D. "Argon Condensation in Free-Jet Expansions." AEDC-TR-74-32 (AD782445), July 1974.
7. Lewis, J. W. L., Williams, W. D., Price, L. L., and Powell, H. M. "Nitrogen Condensation in a Sonic Orifice Expansion Flow." AEDC-TR-74-36 (AD783254), July 1974.
8. Lewis, J. W. L., and Williams, W. D. "Measurement of Temperature and Number Density in Hypersonic Flow Fields Using Laser Raman Spectroscopy." AIAA Paper 75-175, AIAA 13th Aerospace Sciences Meeting, Pasadena, California, January 1975.

9. Ashkenas, H., and Sherman, F. S. "The Structure and Utilization of Supersonic Free Jets in Low Density Wind Tunnels." Rarefied Gas Dynamics, Edited by J. H. de Leeuw, Fourth Symposium, Vol. II., Academic Press, New York, 1966, pp. 84-105.
10. Hilsenrath, J., Beckett, C. W., Benedict, W. S., Fano, L., Hoge, H. J., Masi, J. F., Nuttall, R. L., Touloukian, Y. S., and Woolley, H. W. Tables of Thermal Properties of Gases. National Bureau of Standards Circular 564, Washington, D. C., November 1955.

NOMENCLATURE

D	Orifice diameter
f	Scattering function
I_0	Incident laser intensity
I_s	Scattered intensity
K_α	Optical constant
N	Number density
N_i	Number density of i-mer
P	Pressure
p(i)	Probability distribution function of i-mer
S	Supersaturation parameters defined by Eqs. (9) and (10)
T	Temperature
X_c	Mole fraction of condensate
x, y, z	Directional coordinates
α_i	Polarizability of i-mer

γ Specific heat ratio

λ Wavelength

SUBSCRIPTS

c Condensate

s Saturation value

T Total value

o Reservoir parameter

θ Defined by Eqs. (9) and (10)

ϕ Defined by Eqs. (9) and (10)

∞ Free-stream value

SUPERSCRIPT

0 Isentropic value

Note: Unless otherwise noted, cgs units are used.